

$^{18}\text{O}(^3\text{He}, p)^{20}\text{F}$  reaction and  $(sd)^4$  states in  $^{20}\text{F}^\dagger$ 

D. J. Crozier\* and H. T. Fortune

*Physics Department, University of Pennsylvania, Philadelphia, Pennsylvania 19174*

(Received 10 June 1974)

The  $^{18}\text{O}(^3\text{He}, p)^{20}\text{F}$  reaction has been studied at a  $^3\text{He}$  bombarding energy of 18 MeV. The resulting angular distributions for states of probable  $(sd)^4$  configuration have been examined by the techniques of distorted-wave analysis, utilizing two-particle coefficients of fractional parentage obtained from recent shell-model calculations. Satisfactory agreement is found between theory and the present experiment.

[ NUCLEAR REACTIONS  $^{18}\text{O}(^3\text{He}, p)$ ,  $E = 18.0$  MeV; measured  $\sigma(\theta)$ ; DWBA ]  
analysis with shell-model wave functions.

## I. INTRODUCTION

Although  $^{20}\text{F}$  is in a mass region which has received intensive experimental study, the spins and parities of very few states in this nucleus had been established until recently. Because  $^{20}\text{F}$  is an odd-odd non-self-conjugate nucleus, the structure of its level scheme is very complicated and cannot be interpreted by any simple model. Several theoretical calculations<sup>1-5</sup> have predicted the correct number of states at low excitations in  $^{20}\text{F}$  but have failed to establish a direct correspondence with the experimentally determined levels.

In the last few years, there has been a large increase in experimental interest in  $^{20}\text{F}$ . This upsurge in experimental work has been accompanied and partially instigated by the advent of sophisticated shell-model calculations for the lower part of the  $s$ - $d$  shell.<sup>6</sup> These calculations, which assume an  $^{16}\text{O}$  core and include basis states which span the entire range of  $1d_{5/2}$ - $2s_{1/2}$ - $1d_{3/2}$  orbitals, have attained a great deal of success in describing the properties of low-lying positive-parity states in the mass region  $A = 18$ - $22$ . The nucleus  $^{20}\text{F}$  is the only odd-odd non-self-conjugate nucleus within the range of applicability of the present theoretical computations that can be conveniently studied. Since its structure is far from trivial, it provides a critical test of these calculations. Recently, a study of the  $^{19}\text{F}(d, p)^{20}\text{F}$  reaction<sup>7</sup> has shown that these calculations produced good quantitative agreement with the single-nucleon stripping strengths to low-lying, positive-parity states in  $^{20}\text{F}$ . Two-nucleon-transfer reactions provide an even more sensitive test of the shell-model calculations. Therefore, it was of interest to investigate the  $^{18}\text{O}(^3\text{He}, p)^{20}\text{F}$  reaction and to examine the results in light of the recent theoretical calculations.

## II. EXPERIMENTAL PROCEDURE AND RESULTS

Because elemental oxygen is a gas at all but cryogenic temperatures, the use of oxygen as a target for nuclear research requires the employment of either a gas target chamber or one of the many solid compounds of oxygen. The present experiment used a carbon-backed CaO target.

The 18-MeV beam of  $^3\text{He}$  ions was supplied by the University of Pennsylvania EN tandem Van de Graaff accelerator, and the protons resulting from the  $(^3\text{He}, p)$  reactions were analyzed in a multiangle spectrograph. The protons were detected in nuclear emulsion plates; enough Mylar foil was placed in the focal planes of the spectrograph to stop all other particles. A proton spectrum is displayed in Fig. 1. Several peaks labeled  $^{14}\text{N}$  and  $^{42}\text{Sc}$  are cross hatched in the spectrum; these result, respectively, from the carbon and calcium in the target. The energy resolution is about 40 keV full width at half maximum and results primarily from target thickness and target nonuniformity.

The excitation energies obtained in the present experiment are given in Table I along with literature values from a recent compilation.<sup>8</sup> The quoted errors are standard deviations (the spectrograph had been previously calibrated with a  $^{232}\text{Th}$   $\alpha$  source), and although they are rather small in view of the energy resolution, the excitation energies do agree reasonably well with the literature values.

Absolute cross sections were determined by measuring, at forward angles, the elastic scattering of  $^3\text{He}$  ions by the oxygen in the target, and normalizing to the elastic-scattering cross section predicted by the optical model. They are thought to be accurate to within 50%.

The angular distributions obtained in the present experiment are shown in Figs. 2-9. The curves

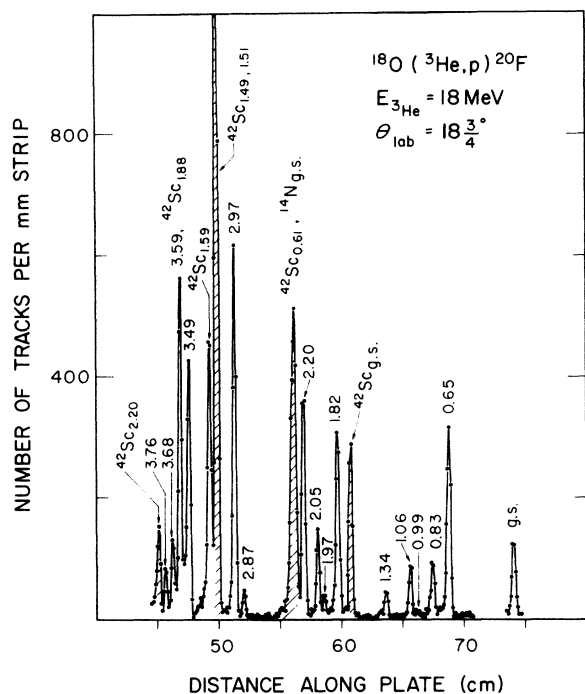


FIG. 1. Representative proton spectrum. The cross-hatched peaks represent proton groups resulting from the  $(^3\text{He}, p)$  reaction on nuclides other than  $^{18}\text{O}$ .

TABLE I. Excitation energies in  $^{20}\text{F}$  (keV).

Present <sup>a</sup>	Literature <sup>b</sup>
0.0	0.0
656.0	655.95 ± 0.15
822.6 ± 1.9	822.9 ± 0.2
983.3 ± 5.3	983.8 ± 0.2
1057.5 ± 2.4	1056.93 ± 0.16
1310.2 ± 3.1	1309.22 ± 0.16
1824.1 ± 3.6	1824.4 ± 1.3
	1843.4 ± 0.3
1978.0 ± 2.8	1970.6 ± 0.3
2044.9 ± 2.2	2043.9 ± 0.3
2194.7 ± 2.8	2193.9 ± 0.3
2863.6 ± 3.9	2865 ± 1.5
2961.4 ± 3.5	2966.2 ± 0.4
3167.2 ± 3.8	3174.6 ± 1.2
3485.9 ± 2.3	3488.4 ± 0.2
	3525.9 ± 0.4
3583.1 ± 2.7	3587.1 ± 0.3
3669.4 ± 4.9	3681.0 ± 0.4
3760 ± 10	3761 ± 2

<sup>a</sup> Quoted errors are measured standard deviations.

<sup>b</sup> Reference 8.

shown in the figure are the results of distorted-wave Born-approximation (DWBA) calculations and will be discussed in the next section.

### III. ANALYSIS

We have analyzed the present data with the DWBA, using two-particle coefficients of fractional parentage<sup>9</sup> (cfp) from the recent shell-model calculations.<sup>6</sup> These cfp are displayed in Table II. The first and second columns of this table list,

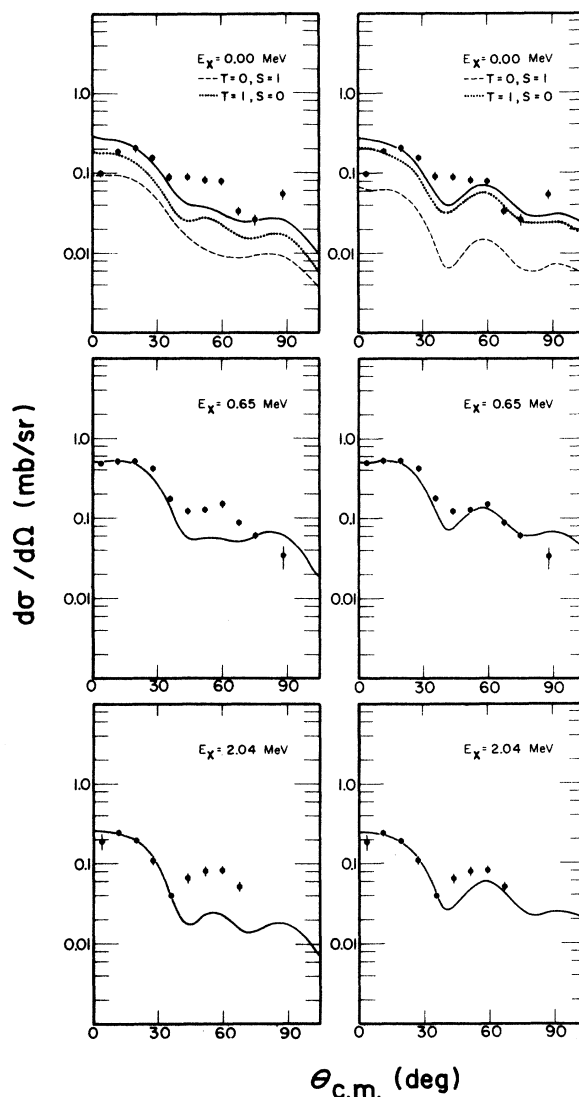


FIG. 2. Angular distributions of states characterized by predominantly  $L=2$  transitions. The solid lines are theoretically predicted distributions. The broken lines for the ground-state transition correspond to the components predicted for the two possible values of the isospin transfer  $T=0$  and  $T=1$ . The left-hand side shows DWBA curves obtained with optical-model potential Set I; the right-hand side, Set II.

respectively, the predicted excitation energies and  $J^\pi$  values of the shell-model states; the subscripts in the second column denote the first or second occurrence of that  $J$  value in the calculations. The third column gives the possible values of orbital angular momentum transfer  $L$  for the given final state  $J^\pi$ . The fourth and fifth columns of the table give the shell-model orbitals into which the two particles are transferred. The next three columns give the transferred values of angular momentum  $J$ , isospin  $T$ , and spin  $S$ . Finally, the last column gives the appropriate two-particle

$^{18}\text{O}(^3\text{He}, p)^{20}\text{F}$ ,  $E_{3\text{He}} = 18.0$  MeV,  $E_x = 0.83$  MeV

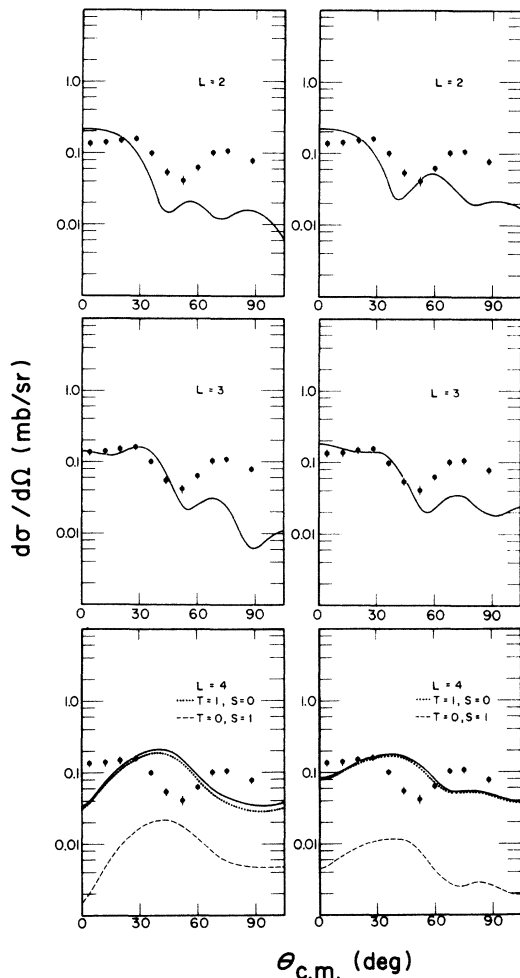


FIG. 3. The angular distribution for the transition to the second excited state of  $^{20}\text{F}$  at 0.83 MeV excitation. At the bottom the calculated curve is the theoretical prediction for the first  $4^+$  state in  $^{20}\text{F}$ . The broken lines are the components predicted for the two possible values of isospin transfer  $T=0$  and  $T=1$ . At the top, a fit to an arbitrarily normalized  $L=2$  distribution is shown. In the center an  $L=3$  fit is shown.

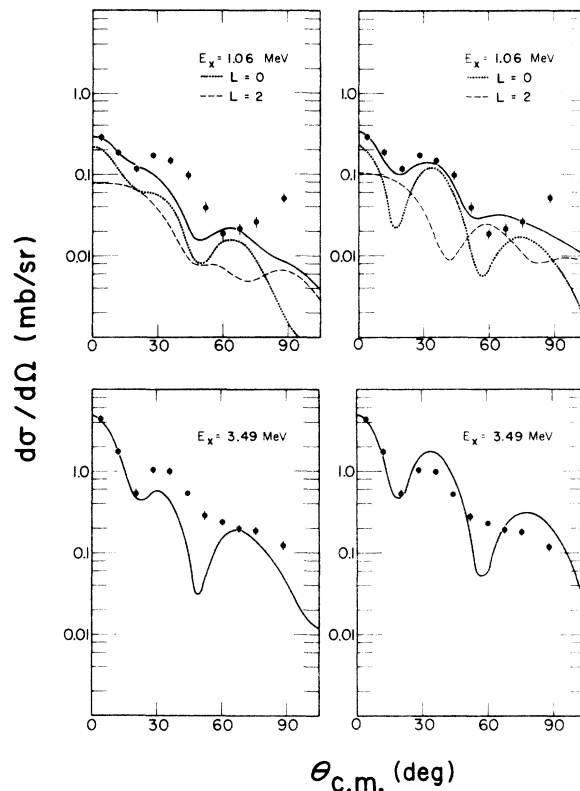


FIG. 4. Angular distributions for the states which exhibit an  $L=0$  component — those at 1.06 and 3.49 MeV excitations. The solid lines are the theoretically predicted cross sections. The broken lines for the 1.06-MeV state are the components for different values of angular momentum transfer  $L=0$  and  $L=2$ . Little  $L=2$  is predicted (or observed) for the 3.49-MeV state.

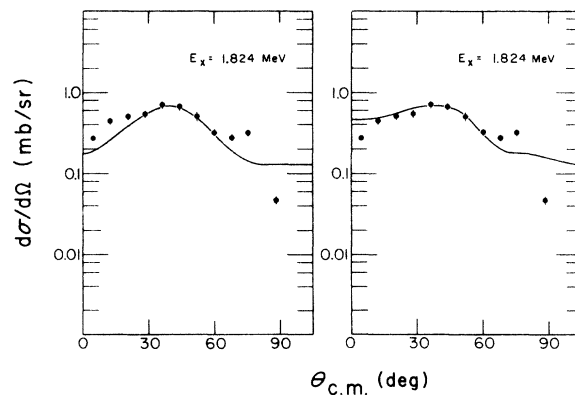


FIG. 5. The predominately  $L=4$  distribution of the transition to the 1.824-MeV level. The solid line represents the theoretical prediction for the first  $5^+$  state in  $^{20}\text{F}$ .

cfp.

The DWBA computations were performed with the two-particle-transfer option of the code DWUCK.<sup>10</sup> Two sets of optical-model parameters were used in analyzing the angular distributions of states with established spin and parity assign-

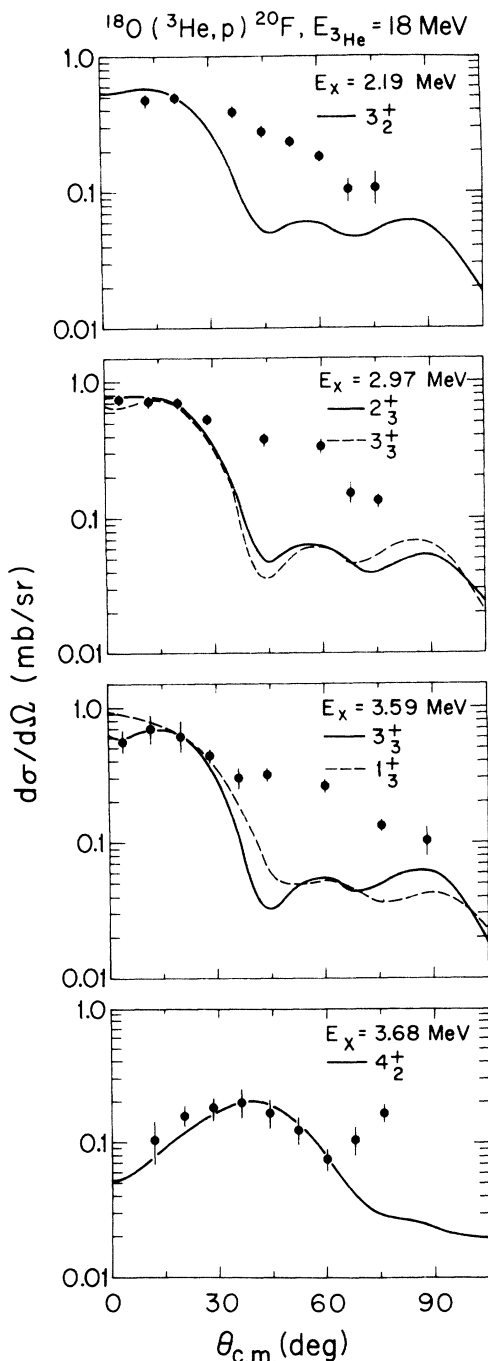


FIG. 6. Angular distributions of four additional positive-parity states whose shell-model correspondences have not yet been established.

ments. These parameters are given in Table III. The  $^3\text{He}$  parameter set, H-I,<sup>11</sup> was used in conjunction with the proton set, P-I,<sup>12</sup> while the  $^3\text{He}$  set, H-II,<sup>13</sup> was used with proton set P-II.<sup>14</sup> Both pairs of potentials have the feature  $r_0(p) \approx r_0(^3\text{He})$  and  $V(^3\text{He}) \approx 3V(p)$ . Potentials that satisfy this "matching" criterion are consistently found to give better agreement between experimental and theoretical angular-distribution shapes than do potentials that do not satisfy the criterion.

The fits to the experimental data obtained using

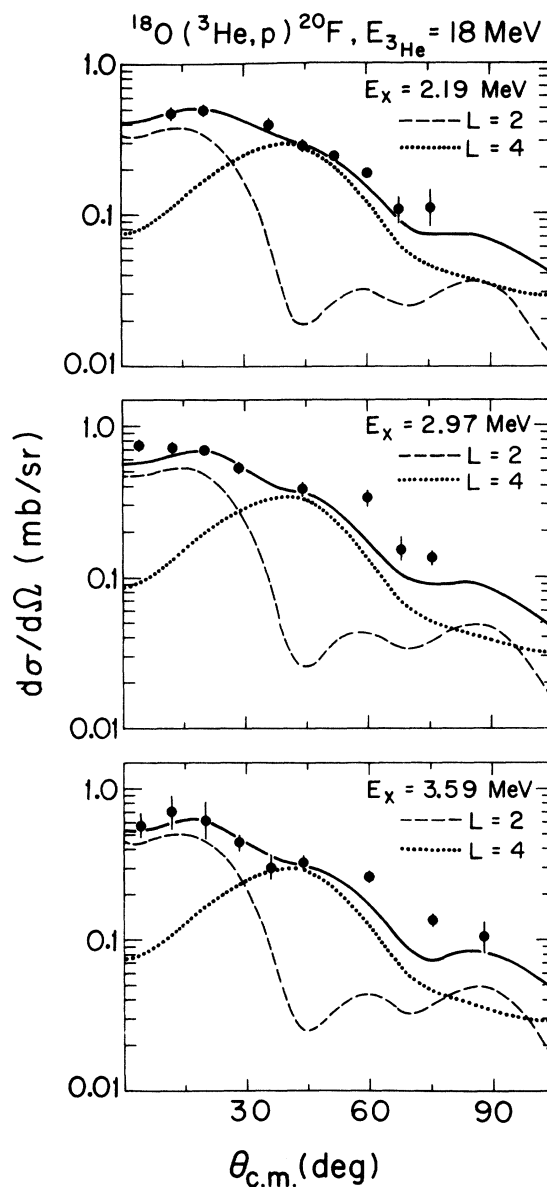


FIG. 7. Angular distributions for the 2.19-, 2.97-, and 3.59-MeV states, together with arbitrarily normalized  $L=2$  and  $4$  DWBA curves. If each is a single state, then these results establish  $J^\pi = 3^+$ .

parameter set I are shown on the left side of Figs. 2-4; those obtained from Set II are shown on the right. In general, calculations with Set II gave better agreement with the data—in both shape and magnitude. In Figs. 6 and 7, which show the fits obtained to positive-parity states that do not have established  $J^\pi$  assignments, only the DWBA calculations employing parameter set II are shown. The broken and dotted lines in Figs. 2-7 are the different components of the angular distributions which are predicted by the theory. For natural-parity states, these correspond to different isospin transfers— $T=0$  or  $T=1$ . For unnatural-parity states they correspond to different  $L$  transfers. For a given state, the admixtures in Figs. 2-6 are those required by the shell-model cfp. The sums

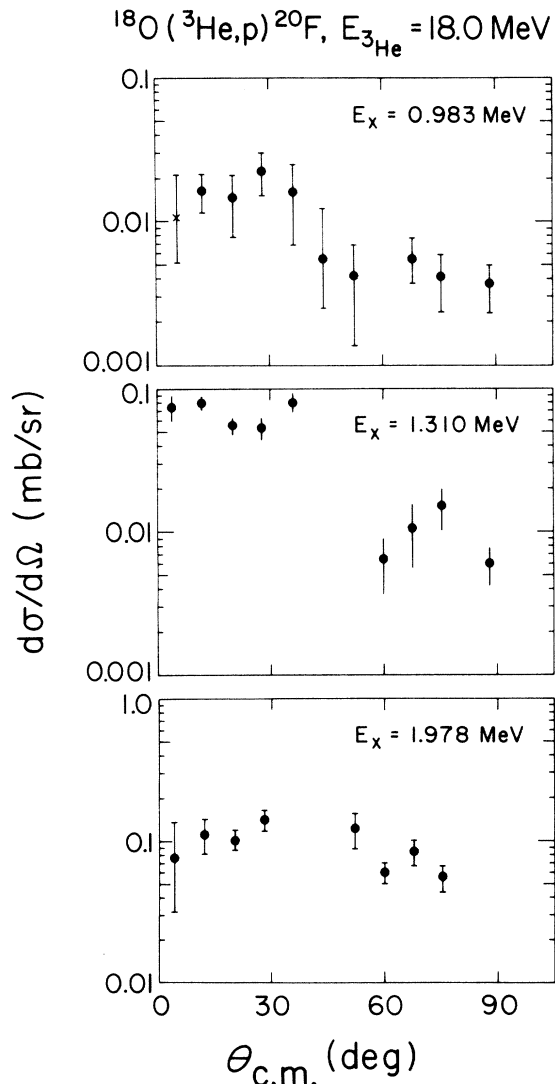


FIG. 8. Angular distributions for low-lying states that have assigned (or suggested) negative parity.

of these components, indicated by solid lines in the figures, have been independently normalized to the experimental data for each state. The normalization factors,  $N = \sigma_{\text{exp}}/\sigma_{\text{th}}$ , thus resulting are given in the last two columns in Table IV. The first two columns of Table IV identify each experimental state by excitation energy and  $J^\pi$ , while the third and fourth indicate the shell-model state with which it has been identified. The results are discussed in the next section.

#### IV. DISCUSSION

In this section we discuss the correspondence between the experimentally known levels of  $^{20}\text{F}$  and the level schemes predicted by three theoretical calculations. This comparison is shown in Fig. 10. In the third column of this figure is the experimental energy-level diagram of  $^{20}\text{F}$ , as determined from this and earlier experimental studies; the spin-parity assignments include those of the present work as discussed below. On the extreme right side of Fig. 10 are presented the results of the shell-model calculations of Halbert *et al.*<sup>6</sup> The lines in the figure indicate the correspondences between experiment and theory. The more certain of these identifications are indicated by solid lines, while the broken lines indicate less certain correspondence. The calculations of Halbert *et al.* treat  $^{20}\text{F}$  as four  $sd$ -shell nucleons outside a closed  $^{16}\text{O}$  core and, hence, do not allow the possibility of negative-parity states. Thus, we have included on the left of Fig. 10 the results of

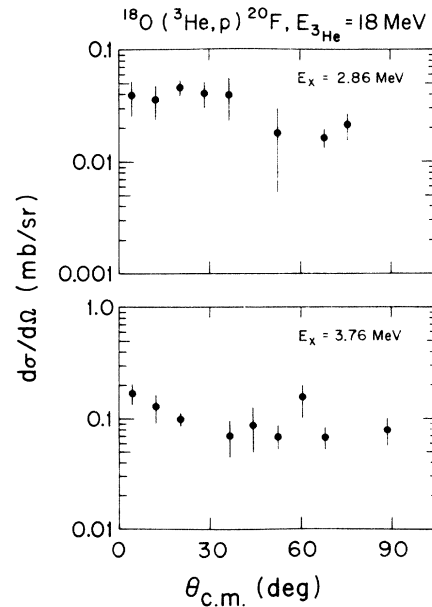


FIG. 9. Angular distributions for two additional states apparently not of  $(sd)^4$  character.

TABLE II. Coefficients of fractional parentage used in distorted-wave calculations.

Excitation	$J^\pi$	$L$	$(nlj)_p$	$(nlj)_n$	$\Delta J$	$\Delta T$	$\Delta S$	cfp
0.0	$2_1^+$	2	$1d_{5/2}$	$2s_{1/2}$	2	0	1	+0.046 666
			$1d_{5/2}$	$1d_{3/2}$	2	0	1	-0.125 345
			$2s_{1/2}$	$1d_{3/2}$	2	0	1	+0.055 394
			$1d_{5/2}$	$1d_{5/2}$	2	1	0	+0.588 746
			$1d_{5/2}$	$2s_{1/2}$	2	1	0	-0.005 376
			$1d_{5/2}$	$1d_{3/2}$	2	1	0	-0.283 956
			$2s_{1/2}$	$1d_{3/2}$	2	1	0	+0.051 067
			$1d_{3/2}$	$1d_{3/2}$	2	1	0	-0.029 851
614	$3_1^+$	2, 4	$1d_{5/2}$	$1d_{5/2}$	3	0	1	+0.024 293
			$1d_{5/2}$	$2s_{1/2}$	3	0	1	-0.198 939
			$1d_{5/2}$	$1d_{3/2}$	3	0	1	-0.051 403
			$1d_{3/2}$	$1d_{3/2}$	3	0	1	-0.012 864
1206	$4_1^+$	4	$1d_{5/2}$	$1d_{3/2}$	4	0	1	-0.146 925
			$1d_{5/2}$	$1d_{5/2}$	4	0	1	+0.724 154
			$1d_{5/2}$	$1d_{3/2}$	4	1	0	-0.083 696
919	$1_1^+$	0, 2	$1d_{5/2}$	$1d_{5/2}$	1	0	1	+0.388 264
			$1d_{5/2}$	$1d_{3/2}$	1	0	1	+0.066 607
			$2s_{1/2}$	$2s_{1/2}$	1	0	1	+0.015 111
			$2s_{1/2}$	$1d_{3/2}$	1	0	1	-0.027 469
			$1d_{3/2}$	$1d_{3/2}$	1	0	1	+0.022 724
2294	$5_1^+$	4	$1d_{5/2}$	$1d_{5/2}$	5	0	1	-0.638 653
1756	$2_2^+$	2	$1d_{5/2}$	$2s_{1/2}$	2	0	1	-0.276 536
			$1d_{5/2}$	$1d_{3/2}$	2	0	1	+0.030 348
			$2s_{1/2}$	$1d_{3/2}$	2	0	1	+0.062 370
			$1d_{5/2}$	$1d_{5/2}$	2	1	0	+0.020 742
			$1d_{5/2}$	$2s_{1/2}$	2	1	0	-0.505 028
			$1d_{5/2}$	$1d_{3/2}$	2	1	0	-0.112 914
			$2s_{1/2}$	$1d_{3/2}$	2	1	0	+0.184 113
			$1d_{3/2}$	$1d_{3/2}$	2	1	0	+0.064 293
2469	$1_2^+$	0, 2	$1d_{5/2}$	$1d_{5/2}$	1	0	1	-0.090 229
			$1d_{5/2}$	$1d_{3/2}$	1	0	1	-0.092 571
			$2s_{1/2}$	$2s_{1/2}$	1	0	1	+0.634 853
			$2s_{1/2}$	$1d_{3/2}$	1	0	1	+0.061 870
			$1d_{3/2}$	$1d_{3/2}$	1	0	1	+0.003 417

TABLE III. Optical-model parameters used in distorted-wave calculations.

Particle	Parameter set	$V$	$r_0$	$a_0$	$W$	$W' = 4W_D$	$r'$	$a_2'$	$V_{so}^a$	$r_{so}$	$a_{so}$	$r_{Coul}$
$^3\text{He}$	H-I <sup>b</sup>	177	1.138	0.7236	18	0	1.602	0.769	5.0	1.138	0.7236	1.40
	H-II <sup>c</sup>	130	1.31	0.7236	18	0	1.602	0.769	5.0	1.138	0.7236	1.40
$p$	P-I <sup>d</sup>	$V_I(p)^e$	$r(p)^f$	0.57	0	$W'(p)^g$	$r(p)^f$	0.5	5.5	$r(p)^f$	0.57	$r(p)^f$
	P-II <sup>h</sup>	$V_{II}(p)^i$	1.25	0.65	0	54.0	1.25	0.47	7.5	1.25	0.65	1.25
Bound state	...	...	1.26	0.60	...	...	...	...	$\lambda=25$	1.26	0.60	1.26

<sup>a</sup> The Program DWUCK takes  $4V_{so}$  for spin  $-\frac{1}{2}$  particles.<sup>b</sup> Reference 11.<sup>c</sup> Reference 13.<sup>d</sup> Reference 12.<sup>e</sup>  $V_I(p) = 60 + 0.04(Z/A^{1/3}) + 27(N-Z)/A - 0.3E$ .<sup>f</sup>  $r(p) = 1.15 - 0.001E$ .<sup>g</sup>  $W'(p) = 4 \times 10(N-Z)/A + 0.64E$  for  $E < 13.8$   
 $= 4 \times 10(N-Z)/A + 9.6 - 0.06E$  for  $E \geq 13.8$ .<sup>h</sup> Reference 14.<sup>i</sup>  $V_{II}(p) = 53.3 - 0.55E + 0.4Z/(A^{1/3}) + 27(N-Z)/A$ .

TABLE IV. Comparison of experimental and theoretical states.

Experimental		Shell model		$\sigma_{\text{exp}}/\sigma_{\text{DWBA}} \times 10^3$	
Exc. (keV)	$J^\pi$	Exc. (keV)	$J^\pi$	Set I	Set II
0	$2^+$	0	$2^+$	0.46	0.51
656	$3^+$	614	$3^+$	0.71	0.83
823	$4^+$	1206	$4^+$	0.22	0.36
1057	$1^+$	919	$1^+$	1.16	1.03
1824	$5^+$	2294	$5^+$	0.32	0.48
2045	$2^+$	1756	$2^+$	0.80	1.15
3486	$1^+$	2469	$1^+$	0.69	0.69

two other recent theoretical calculations for the negative-parity states. The calculations of Wildenthal,<sup>15</sup> shown at the left center of Fig. 10, are similar to those of Halbert *et al.*,<sup>6</sup> but allow up to four holes in the  $1p_{1/2}$  shell and do not include the

$1d_{3/2}$  orbital. On the far left of Fig. 10, we present the results of a recent calculation by Johnstone, Castel, and Sostegno<sup>5</sup> for the negative-parity states of  $^{20}\text{F}$ . These calculations consider the coupling of low-lying positive-parity states in  $^{21}\text{Ne}$  to proton hole states in the  $1p$  shell.

The following discussion draws heavily upon the results of earlier experimental studies of  $^{20}\text{F}$ <sup>7,16-27</sup> in attempting to identify the experimental states with appropriate shell-model counterparts.

A. States at 0.00, 0.66, and 2.04 MeV excitation

The angular distributions of three low-lying states in  $^{20}\text{F}$ —the ground state and states at  $E_x = 0.66$  and 2.04 MeV—are characterized predominantly by  $L=2$  distributions. These angular distributions are displayed in Fig. 2.

The ground state of  $^{20}\text{F}$  is known to have spin and parity  $2^+$ .<sup>8</sup> The lowest level predicted by the shell

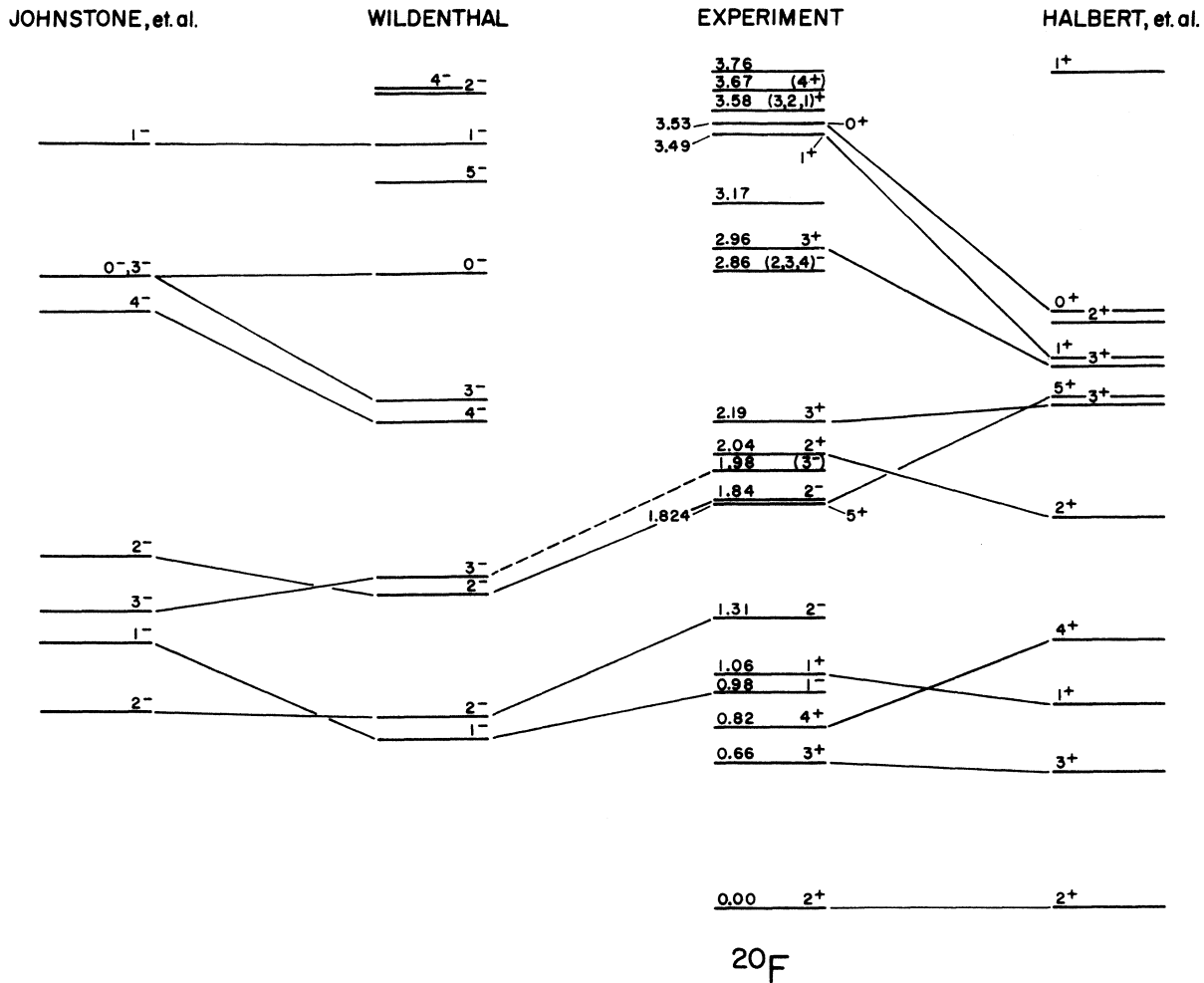


FIG. 10. Comparison of experimental and theoretical level schemes of  $^{20}\text{F}$ .

model is also  $2^+$ , and this correspondence has been assumed in Table IV. The ratio  $\sigma_{\text{exp}}/\sigma_{\text{th}}$  given in Table IV for this state is in reasonable agreement with the values for the other states for which corresponding shell-model states have been assigned. The predicted angular distribution gives only a fair fit to the experimentally measured one.

The first excited state of  $^{20}\text{F}$  at 0.66 MeV excitation also exhibits a predominately  $L=2$  angular distribution. This state has been observed to decay to the  $2^+$  ground state of  $^{20}\text{F}$ <sup>16,17,19,23</sup> and particle- $\gamma$  correlation measurements<sup>16</sup> and the measured lifetime of  $370 \pm 60$  fs<sup>23</sup> and  $359_{-39}^{+51}$  fs<sup>19</sup> strongly imply  $J^\pi = 3^+$ . This state is also seen to have a large  $l_n=2$  strength in the  $^{19}\text{F}(d,p)^{20}\text{F}$  reaction.<sup>7</sup> A study of the  $^{19}\text{F}(d,p)^{20}\text{F}$  reaction with polarized deuterons<sup>28</sup> has firmly established its  $J^\pi$  as  $3^+$ . The first excited state of  $^{20}\text{F}$  is predicted by the shell model to be  $3^+$  and therefore this theoretical state is identified with the experimental state at 0.66 MeV. Indeed, the ratio  $\sigma_{\text{exp}}/\sigma_{\text{th}}$  obtained from this assignment given in Table IV, is in good agreement with the values obtained for other states with reasonably certain shell-model counterparts. The spin-parity assignment of  $3^+$  is therefore further substantiated by the present investigation.

The third state, at 2.04 MeV excitation, that possesses a predominately  $L=2$  angular distribution is also observed in the  $^{19}\text{F}(d,p)^{20}\text{F}$  reaction to have a large  $l_n=2$  strength.<sup>7</sup> This state has been observed to decay to the  $3^+$  state at 0.66 MeV and to the  $2^+$  ground state.<sup>17,19,20,21</sup>  $\gamma$ -correlation studies<sup>25</sup> in combination with the measured lifetime  $37 \pm 16$  fs<sup>23</sup> indicate an unequivocal assignment of  $2^+$  for this state. The theoretical calculations being considered here suggest only one  $2^+$  state in this region of excitation, which we therefore identify with the observed state at 2.04 MeV. The ratio,  $\sigma_{\text{exp}}/\sigma_{\text{th}}$ , obtained by this identification and given in Table IV, is among the larger values obtained from the more certain identifications of experimental and theoretical states, but is not unreasonable.

#### B. States at 1.06 and 3.49 MeV excitation

The angular distributions of the states at 1.06 and 3.49 MeV excitation, which are shown in Fig. 3, exhibit significant  $L=0$  components. The 1.06-MeV state has been observed to decay to the  $2^+$  ground state<sup>17,19,20,21,25</sup> and has a lifetime of  $45 \pm 13$  fs.<sup>8</sup> A directional correlation study<sup>18</sup> suggests  $J=1$ , which is consistent with an early  $1^+$  assignment based on the  $\beta$  decay of  $^{20}\text{O}$ .<sup>29</sup> The observation of a weak  $l_n=0$  transition to this state in the  $^{19}\text{F}(d,p)^{20}\text{F}$  reaction is consistent with an identifi-

cation with the first  $1^+$  state predicted by the shell-model calculations. The observation of a mixed  $L=0$  and  $L=2$  transitions in the  $^{18}\text{O}(^3\text{He},p)^{20}\text{F}$  reaction is consistent only with a  $1^+$  assignment. The identification of this state with the first shell-model  $1^+$  state has therefore been made and the values of  $\sigma_{\text{exp}}/\sigma_{\text{th}}$ , given in Table IV, are in reasonable agreement with those for the other states.

The observed  $L=0$  transition to the 3.49-MeV state in the  $^{18}\text{O}(^3\text{He},p)^{20}\text{F}$  reaction implies a  $J^\pi$  assignment of  $0^+$  or  $1^+$  to this state. Although no significant  $L=2$  admixture is predicted for the second shell-model  $1^+$  state and none seems required in order to fit the angular distribution, the absence of a deep minimum at about  $50^\circ$  which is characteristic of  $0^+ \rightarrow 0^+$  transitions in this mass region<sup>30</sup> may be taken as evidence that the spin of this state is 1. This state decays to the ground state and to the states at 0.98, 1.06, 1.31, and 1.84 MeV excitation,<sup>20,21</sup> with a lifetime of  $44 \pm 11$  fs.<sup>23</sup> The strength of the  $l_n=0$  transition to this state observed in the  $^{19}\text{F}(d,p)^{20}\text{F}$  reaction also indicates that its  $J^\pi$  is  $1^+$ .<sup>8</sup> Probably the strongest argument for a  $1^+$  spin assignment, however, is the significant strength of this state in the  $^{22}\text{Ne}(d,\alpha)^{20}\text{F}$  reaction.<sup>26</sup> The ratio  $\sigma_{\text{exp}}/\sigma_{\text{th}}$  obtained by the identification of the 3.49-MeV state as the second  $1^+$  state predicted by the shell model is in agreement with that obtained for other states.

The  $0^+$  state at 3.53 MeV was not populated with sufficient strength to allow an angular distribution to be extracted.

#### C. State at 1.824 MeV excitation

The state at 1.824 MeV is one member of a doublet; the other member lying at 1.843 MeV excitation. The decay of this state has been determined to be predominately to the state at 0.82 MeV.<sup>25</sup> In early studies<sup>16,20</sup> of the decay a branch to the ground state was reported, but this doublet was not resolved. In more recent work<sup>31</sup> no ground-state branch was observed. From directional correlation measurements of the branch to the 0.82-MeV state, Quin *et al.* suggest  $J=1, 2,$  or  $3$  for the 1.824-MeV state if the spin of the 0.82-MeV state is 2. (Present experimental evidence restricts  $J^\pi = 2$  or  $4$  for the 0.82-MeV state. This point will be discussed subsequently.) If, on the other hand, the 0.82-MeV state has spin 4, they favor  $J=3$  or  $5$  for the 1.824-MeV state, with slight preference for  $J=3$ . The  $^{18}\text{O}(^3\text{He},p)^{20}\text{F}$  angular distribution is shown in Fig. 4. It is apparent that the distribution is predominately  $L=4$ . This fact, in combination with the results of Quin *et al.*, limits the possible spin-parity assignments for this state to  $3^+$  and  $5^+$ . The absence of any



significant  $L=2$  strength in the angular distribution, however, makes a  $3^+$  assignment unlikely since  $0^+ \rightarrow 3^+$  transitions in this region generally exhibit a prominent  $L=2$  component. Recent work<sup>32</sup> leads to a more model-independent assignment of  $J^\pi = 5^+$ . We have therefore identified the 1.824-MeV state with the  $5^+$  state predicted by the shell model to lie in this region of excitation. The ratio  $\sigma_{\text{exp}}/\sigma_{\text{th}}$  obtained from this identification is given in Table IV and is in reasonable agreement with values of this ratio obtained for other states.

#### D. State at 0.82 MeV excitation

The second excited state of  $^{20}\text{F}$  poses an interesting puzzle. Recent correlation studies<sup>25,27</sup> of the decay of this state have limited the possible spin assignment to 2 or 4, but among the corroborating experimental evidence there are data which appear to substantiate each of these values to the exclusion of the other. The most important support for a  $2^+$  assignment is an apparent  $l_n=2$  transition observed in the  $^{19}\text{F}(d, p)^{20}\text{F}$  reaction.<sup>33</sup> In a more recent investigation of this reaction, however, Fortune *et al.*<sup>7</sup> point out that an assumption of  $l_n=2$  transfer yields spectroscopic strengths that are drastically different for bombarding energies of 8.9 MeV<sup>33</sup> and 16 MeV.<sup>7</sup> This result is suggestive of a nondirect reaction mechanism, and casts doubt on the earlier<sup>33</sup>  $l_n=2$  assignment.

There is other evidence in the literature which favors the  $4^+$  assignment. Hardell and Hasselgren,<sup>18</sup> for example, failed to observe any direct  $\gamma$  transition to this level from the 6.602-MeV neutron capture level. Such a decay would be expected for a  $2^+$  state. Furthermore, the 11.08-MeV state in  $^{20}\text{Ne}$  has been given the tentative assignment ( $4^+$ ),  $T=1$ . If this assignment is correct, it would require the existence of a  $4^+$  state near 0.8 MeV in  $^{20}\text{F}$ . The present shell-model calculations also predict a low-lying  $4^+$  state (at 1.203 MeV). All of the other experimentally known states below 2 MeV excitation have been determined not to be  $4^+$ , and thus the 0.82-MeV level is the only possible candidate. Quin *et al.* indicate that if  $J^\pi$  is  $2^+$  for the 0.82-MeV state, then their  $E2/M1$  mixing ratio for the ground-state decay,<sup>25</sup> in conjunction with the lifetime measurement,  $76 \pm 2$  ps, of Nickles,<sup>22</sup> implies an  $M1$  hindrance factor two orders of magnitude greater than is customarily observed in this region. They therefore favor a  $J=4$  assignment. A more recent measurement of this lifetime<sup>27</sup> yielded  $\tau = 79 \pm 6$  ps, in good agreement with the earlier value. Finally, if the 1.824-MeV state has  $J^\pi = 5^+$ , the spin of the 0.82-MeV state must be 4, as mentioned earlier.

The angular distribution observed for the 0.82-

MeV state in the  $^{18}\text{O}(^3\text{He}, p)^{20}\text{F}$  reaction is displayed in Fig. 5. As can be seen at the bottom of Fig. 5, the agreement between this distribution and the theoretical curve predicted for the first  $4^+$  state is disappointingly poor. Also, the ratio  $\sigma_{\text{exp}}/\sigma_{\text{th}}$  resulting from this identification is the least consistent of the values obtained for all the low-lying states. At the top of Fig. 5 the angular distribution of the 0.82-MeV state is compared with an arbitrarily normalized  $L=2$  DWBA calculation. It is obvious that the observed distribution cannot be satisfactorily fitted with calculations commensurate with either a  $2^+$  or a  $4^+$  assignment. In the center of Fig. 5, a fit to an arbitrarily normalized  $L=3$  distribution is shown. This DWBA calculation produces the best fit to the forward-angle data, thus suggesting the disturbing possibility that this state has negative parity.

Our inability to fit the angular distribution of the 0.82-MeV state satisfactorily by assuming  $L=4$  transfer is somewhat disappointing and not understood. We nevertheless feel that a  $4^+$  assignment should be favored. Quin *et al.* point out that a  $5^+$  assignment for the 1.82-MeV state is possible only if the spin of the 0.82-MeV state is 4 and it now appears<sup>32</sup> that the 1.82-MeV state indeed has  $J^\pi = 5^+$ . Thus, despite the poor fit obtained in the present work for  $L=4$ , the spin-parity of the 0.82-MeV state is most likely  $4^+$ .

#### E. States at 0.98, 1.31, and 1.98 MeV excitation

The angular distributions of the three low-lying states at 0.98, 1.31, and 1.98 MeV excitation are shown in Fig. 8. These states are only weakly populated in the  $^{18}\text{O}(^3\text{He}, p)^{20}\text{F}$  reaction and their differential cross sections show no easily recognizable shape. Because of their weak cross sections, no attempt has been made to fit the angular distributions of these states. It has been suggested from the results of the  $^{22}\text{Ne}(d, \alpha)^{20}\text{Ne}$  reaction<sup>24</sup> that these states all have negative parity. In fact,  $\gamma$ -ray polarization measurements<sup>32,34</sup> have recently established that the 0.98-MeV state has  $J^\pi = 1^-$  and that the 1.31-MeV state has  $J^\pi = 2^-$ . The 1.98-MeV state has a probable  $3^-$  assignment.<sup>35,36</sup> Possible correspondence with predicted negative-parity states are shown in Fig. 10.

#### F. States at 2.19, 2.96, 3.58, and 3.67 MeV excitation

There are four other positive-parity states in  $^{20}\text{F}$  which were observed in the present experiment. However, shell-model counterparts for these four states cannot be firmly established. The angular distributions for these levels together with theoret-

ically predicted cross sections for various possible shell-model counterparts are shown in Figs. 6 and 7. (These theoretical distributions have been calculated with the second set of optical-model parameters only.) For three of these states—those at 2.19, 2.96, and 3.58 MeV excitation—the angular distributions shown in Fig. 7 have been fitted with arbitrary mixtures of  $L=2$  and  $L=4$ .

The state at 2.19 MeV has been observed to decay to the ground state as well as to the second state at 0.82 MeV excitation.<sup>18,20,21,23,25,36</sup> Correlation measurements<sup>25,36</sup> of these decays limit the possible spin assignments for this state to  $J=1$ , 2, or 3. In addition, if the spin of the 0.82-MeV state is  $4^+$ , as appears likely, these correlation measurements allow only  $J=3$ .<sup>36</sup> An  $l_n=2$  transition to this state observed in the  $^{19}\text{F}(d,p)^{20}\text{F}$  reaction<sup>7</sup> indicates that the 2.19-MeV state has positive parity. In Fig. 6, the angular distribution of the 2.19-MeV state is fitted with the theoretical prediction for the second  $3^+$  state predicted by the shell model. The poor fit at larger angles may be attributed to a deficiency of  $L=4$  strength in the theoretical prediction. It can be seen in Fig. 7 that an arbitrary mixture of  $L=2$  and  $L=4$  fits this distribution well. For a single state, this admixture requires a  $3^+$  assignment.

The state at 2.96 MeV has been observed to decay to the ground state and to the 0.823-MeV state<sup>18-21,23,25</sup> and to the 0.66- and 1.98-MeV states.<sup>36</sup> Correlation measurements<sup>25,36</sup> of the decay to the 0.82-MeV state together with the measured lifetime,  $60 \pm 40$  fs,<sup>23</sup> indicate a  $J=3$  assignment for this state if the 0.82-MeV state is  $4^+$ . An observed  $l_n=2$  transition in the  $^{19}\text{F}(d,p)^{20}\text{F}$  reaction<sup>7</sup> indicates that this state has positive parity. In Fig. 6 the angular distribution is shown with fits corresponding to the third  $2^+$  and third  $3^+$  states predicted by the shell model. As can be seen, the predominately  $L=2$  transitions predicted by the shell model for these theoretical states fail to fit the experimental data at back angles. This can again be considered as a deficiency in  $L=4$  strength and, as can be seen in Fig. 7, an arbitrary mixture of  $L=2$  and  $L=4$  is capable of fitting the differential cross section—as would be expected for a  $3^+$  assignment.

The state at 3.58 MeV decays to the ground state and 2.04-MeV excited state<sup>17,20,21,23</sup> as well as to the 0.66- and 1.06-MeV states.<sup>18</sup> Its lifetime has been measured as  $30 \pm 30$  fs.<sup>23</sup> A predominate  $l_n=2$  transition (with a hint of  $l_n=0$ ) has been observed to this state in the  $^{19}\text{F}(d,p)^{20}\text{F}$  reaction.<sup>7</sup> The angular distribution of this state is shown in Fig. 6 together with the theoretical predictions for the third  $1^+$  and third  $3^+$  states of the shell model. In Fig. 7 it can be seen that this state is better

fitted with a larger  $L=4$  component. The fact that this distribution can be fitted with a mixed  $L=2$  and  $L=4$  calculation is indicative of a  $3^+$  spin-parity assignment for the 3.58-MeV state, if it is indeed a single state.

Decays of the 3.67-MeV state to the ground state and to the first excited state at 0.66 MeV have been observed.<sup>20</sup> It is weakly populated in the  $^{19}\text{F}(d,p)^{20}\text{F}$  reaction.<sup>7</sup> It is populated in  $^{18}\text{O}(^3\text{He},p)^{20}\text{F}$  by an  $L=4$  distribution, which has been compared in Fig. 6 with the theoretical distribution corresponding to the second  $4^+$  shell-model state. The most probable  $J^\pi$  assignment for this state is thus  $4^+$ .

#### G. States at 2.86 and 3.76 MeV excitation

The angular distributions for the remaining two states observed in the present experiment are shown in Fig. 9. The cross sections for the transitions to the 2.86- and 3.76-MeV states are small and the shapes are nondescript. These two states are likely to be negative-parity states, but little additional information about these levels is known. The 2.86-MeV state has been observed to decay to the ground state<sup>25,36</sup> and is very weakly populated in the  $^{19}\text{F}(d,p)^{20}\text{F}$  reaction.<sup>7</sup> A possible decay of the 3.76-MeV state to the 0.66-MeV state has been suggested.<sup>36</sup>

#### V. CONCLUSION

With the recently increasing attention devoted to  $^{20}\text{F}$ , it is becoming possible to identify most of the low-lying states in this nucleus with the  $(sd)^4$  states predicted by the shell-model calculations of Halbert *et al.*,<sup>6</sup> as may be seen in Fig. 10. In addition, Fig. 10 shows that it is plausible to assume that an association between the observed negative-parity states and the predictions of Wildenthal<sup>15</sup> and of Johnstone *et al.*<sup>5</sup> does, indeed, exist, although the available experimental information on these states is insufficient for a precise identification. We have observed that for many of the low-lying states the shell-model calculations of Halbert *et al.*<sup>6</sup> accurately predict the relative strengths—even the relative strengths of different  $L$  values whenever more than one orbital angular momentum transfer is possible. They predict the relative cross sections of different  $(sd)^4$  states correctly to within a factor of 3 in Table IV. Thus, it is evident that the sophistication of modern theoretical calculations is becoming sufficient to compute with reasonable accuracy the properties of nuclear systems as complicated as  $^{20}\text{F}$ . They should prove useful in the future interpretation of nuclear phenomena in the  $2s-1d$  shell.

## ACKNOWLEDGMENTS

The assistance of J. R. Powers in data accumulation is appreciated. The target was prepared by L. Csihas. We acknowledge interesting and infor-

mative discussions with P. R. Chagnon, E. C. Halbert, K. Hardy, J. B. McGrory, J. G. Pronko, P. A. Quin, and B. H. Wildenthal. We are grateful to J. B. McGrory for providing the two-particle cfp's.

- <sup>†</sup>Work supported by the National Science Foundation.  
<sup>\*</sup>Present address: Department of Physics, Kansas State University, Manhattan, Kansas 66502.
- <sup>1</sup>S. Cohen, E. C. Halbert, and S. P. Pandya, Nucl. Phys. A114, 353 (1968).  
<sup>2</sup>A. Arima, S. Cohen, R. D. Lawson, and M. H. Macfarlane, Nucl. Phys. A108, 94 (1968).  
<sup>3</sup>E. C. Halbert, J. B. McGrory, and B. H. Wildenthal, Phys. Rev. Lett. 20, 1112 (1968).  
<sup>4</sup>R. J. W. Hodgson, Can. J. Phys. 47, 2269 (1969).  
<sup>5</sup>I. P. Johnstone, B. Castel, and P. Sostegno, Phys. Lett. 34B, 34 (1971).  
<sup>6</sup>E. C. Halbert, J. B. McGrory, B. H. Wildenthal, and S. P. Pandya, *Advances in Nuclear Physics* (Plenum, New York, 1971), Vol. 4.  
<sup>7</sup>H. T. Fortune, G. C. Morrison, R. C. Bearse, J. L. Yntema, and B. H. Wildenthal, Phys. Rev. C 6, 21 (1972).  
<sup>8</sup>F. Ajzenberg-Selove, Nucl. Phys. A190, 1 (1972).  
<sup>9</sup>J. B. McGrory, private communication.  
<sup>10</sup>We are grateful to Dr. P. D. Kunz for making this program available to us.  
<sup>11</sup>H. T. Fortune, N. G. Puttaswamy, and J. L. Yntema, Phys. Rev. 185, 1546 (1969).  
<sup>12</sup>B. A. Watson, P. P. Singh, and R. E. Segel, Phys. Rev. 182, 977 (1969).  
<sup>13</sup>H. Kattenborn, C. Mayer-Boricke, and B. Mertens, Nucl. Phys. A138, 657 (1969).  
<sup>14</sup>F. G. Perey, Phys. Rev. 131, 745 (1963).  
<sup>15</sup>B. H. Wildenthal, private communication.  
<sup>16</sup>G. A. Bissinger, R. M. Mueller, P. A. Quin, and P. R. Chagnon, Nucl. Phys. A90, 1 (1967).  
<sup>17</sup>I. Bergqvist, J. A. Biggerstaff, J. H. Gibbons, and W. M. Good, Phys. Rev. 158, 1049 (1967).  
<sup>18</sup>R. Hardell and A. Hasselgren, Nucl. Phys. A123, 215 (1969).  
<sup>19</sup>R. L. Hershberger, M. J. Wozniak, Jr., and D. J. Donahue, Phys. Rev. 186, 1167 (1969).  
<sup>20</sup>P. Spilling, H. Gruppelaar, H. F. De Vries, and A. M. J. Spits, Nucl. Phys. A113, 395 (1968).  
<sup>21</sup>T. Holtebekk, S. Tryti, and G. Vamraak, Nucl. Phys. A134, 353 (1969).  
<sup>22</sup>R. J. Nickles, Nucl. Phys. A134, 308 (1969).  
<sup>23</sup>T. Holtebekk, R. Stromme, and S. Tryti, Nucl. Phys. A142, 251 (1970).  
<sup>24</sup>H. T. Fortune, J. D. Garrett, P. Neogy, and R. Middleton, Bull. Am. Phys. Soc. 15, 36 (1970); and to be published.  
<sup>25</sup>P. A. Quin, G. A. Bissinger, and P. R. Chagnon, Nucl. Phys. A155, 495 (1970).  
<sup>26</sup>H. T. Fortune, J. D. Garrett, J. R. Powers, and R. Middleton, Phys. Rev. C 4, 850 (1971).  
<sup>27</sup>J. G. Pronko and R. W. Nightingale, Phys. Rev. C 4, 1023 (1971).  
<sup>28</sup>P. A. Quin and S. E. Vigdor, Bull. Am. Phys. Soc. 15, 1686 (1970).  
<sup>29</sup>G. Scharff-Goldhaber, A. Goodman, and M. G. Silbert, Phys. Rev. Lett. 4, 25 (1960).  
<sup>30</sup>R. R. Betts, H. T. Fortune, J. D. Garrett, R. Middleton, D. J. Pullen, and O. Hansen, Phys. Rev. Lett. 26, 1121 (1971).  
<sup>31</sup>L. A. Alexander, W. K. Collins, B. P. Hichwa, J. C. Lawson, D. S. Longo, E. D. Berners, and P. R. Chagnon, Phys. Rev. C 6, 817 (1972).  
<sup>32</sup>D. S. Longo, J. C. Lawson, L. A. Alexander, B. P. Hichwa, and P. R. Chagnon, Phys. Rev. C 8, 1347 (1973).  
<sup>33</sup>F. A. El Bedewi, Proc. Phys. Soc. (Lond.) A69, 221 (1956).  
<sup>34</sup>K. A. Hardy and Y. K. Lee, Phys. Rev. C 7, 1441 (1973).  
<sup>35</sup>J. N. Bishop and H. T. Fortune, Bull. Am. Phys. Soc. 18, 678 (1973).  
<sup>36</sup>J. G. Pronko, Phys. Rev. C 7, 127 (1973).